Biophysical Journal, Volume *114*

Supplemental Information

Insights into the Aggregation Mechanism of PolyQ Proteins with Different Glutamine Repeat Lengths

Tetyana Yushchenko, Elke Deuerling, and Karin Hauser

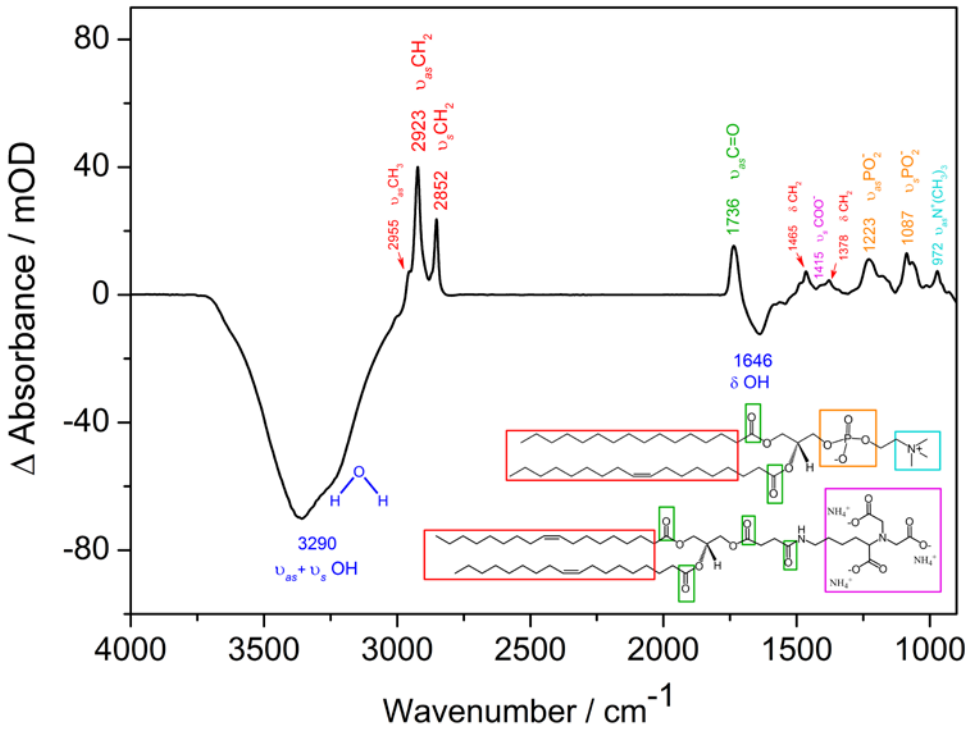

Figure S1. IR difference spectrum of lipid bilayer (LB) formation. Vesicles were produced with a lipid mixture of POPC (upper structure) and NTA-DOGS (lower structure). After vesicle spreading on the activated Ge internal reflection element (IRE), the formation of the bilayer was monitored by ATR-FTIR. The positive bands result from the absorption of the functional groups of the LB while the negative bands (at 3290 cm^{-1} and 1646 cm^{-1}) show the displaced H_2O molecules of the buffer. Lipid bands increase with time as the bilayer forms on the IRE surface. The bands are from the asymmetric (2923 cm^{-1}) and the symmetric (2852 cm^{-1}) stretching vibrations of methylene CH_2. The band at 1736 cm^{-1} is from the carbonyl groups. The carboxyl groups of NTA give signal at 1415 cm^{-1} and the phosphate groups absorb at 1223 cm^{-1} and 1087 cm^{-1}. The lipid bilayer was completely formed after 10 min incubation. Gently flushing with the buffer removed unbound lipid vesicles. The lipid bilayer was used for construct immobilization and its spectrum subtracted as background after initiation of the polyQ aggregation process by enzymatic cleavage.

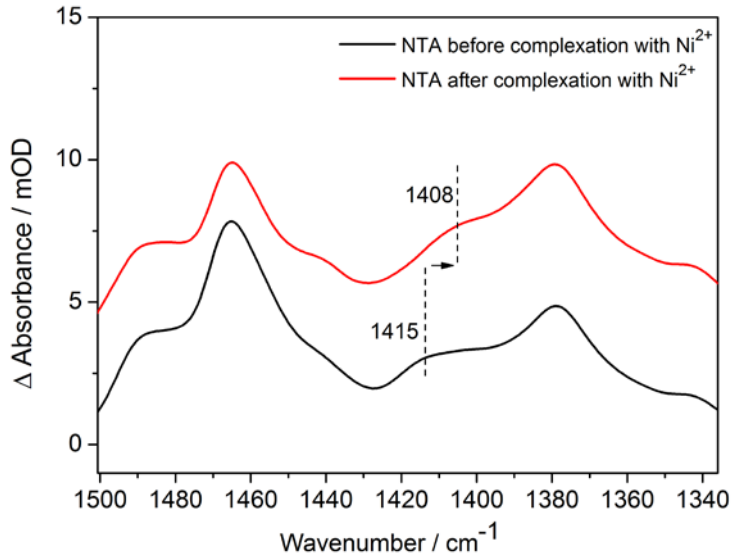

Figure S2. Comparison of the IR spectra of NTA groups before (black) and after (red) incubation with Ni^{2+} ions. In order to form a tetradentate complex NTA with Ni^{2+}, 5mM $NiCl_2$ in lipid buffer was added to the already formed LB and incubated for 1h. Due to the small concentration of NTA groups on the LB, the complexation process leads to minor spectral changes. Nevertheless, a band shift from 1415 cm^{-1} (black spectrum, vacant NTA groups) to 1408 cm^{-1} (red spectrum, Ni^{2+} bound NTA) is observed as expected (1).

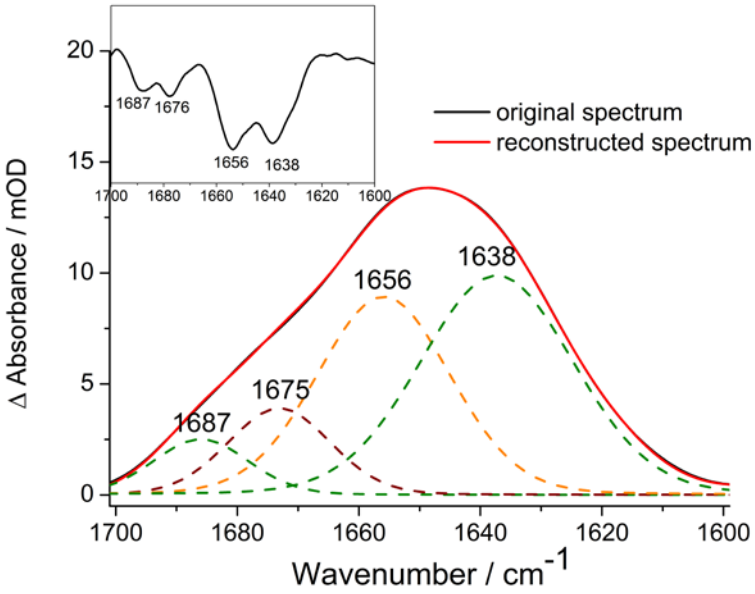

Figure S3. Curve-fitting and amide I components of the SUMO protein. SUMO was immobilized on the LB via its His-tag. The absorption bands at 1638 cm^{-1}/1687 cm^{-1} reveal the antiparallel β-sheets and the band at 1656 cm^{-1} the α-helices of SUMO. Turn and loop structures are indicated by the band at 1675 cm^{-1}. The second-derivative spectrum (inset) reveals the peak positions of the amide I components used in the curve-fitting procedure. Prior to the SUMO immobilization, the spectrum of the LB with the H_2O/buffer was subtracted as background. The IR secondary structure analysis agrees reasonably well with the high-resolution structure determined by NMR (2).

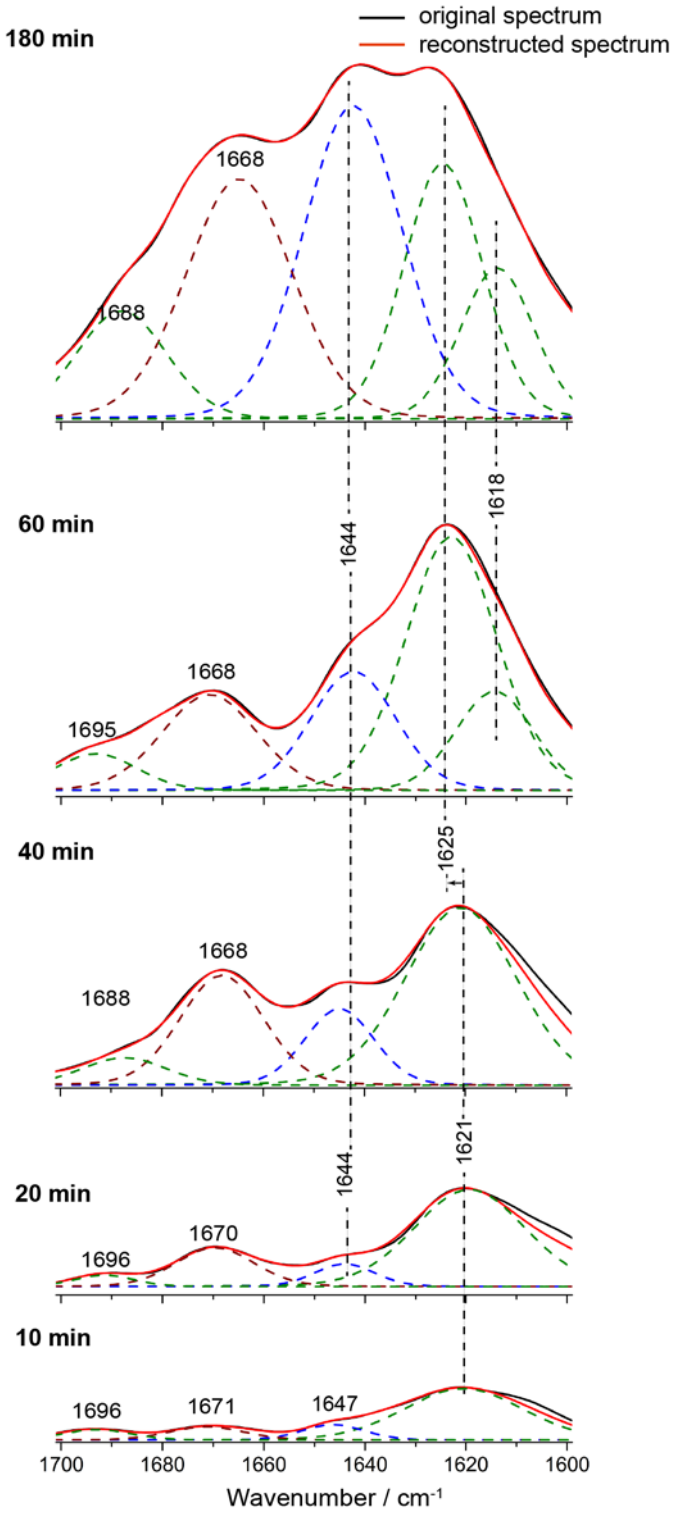

Figure S4. Curve-fitting and amide I components of N17-Q11-Flag in dependence of time (10 min, 20 min, 40 min, 60 min and 180 min after enzymatic cleavage with Ulp1). The spectra show the structural transitions of the N17-Q11-Flag fragments. Frequency positions below 1630 cm^{-1} indicate β-structured aggregates. The occurrence of several components below 1630 cm^{-1} hints at the heterogeneity of β-structured aggregates which develop over time. The weak bands at 1696/1688 cm^{-1} reveal the antiparallel organization of the β-strands. The stretches are too short to form intramolecular β-sheets (no band 1630 – 1640 cm^{-1}). The intensities of the components show that a significant fraction of disordered structure (1647/1644 cm^{-1}) as well as loop/turns (1672-1668 cm^{-1}) are also present in the final aggregates.

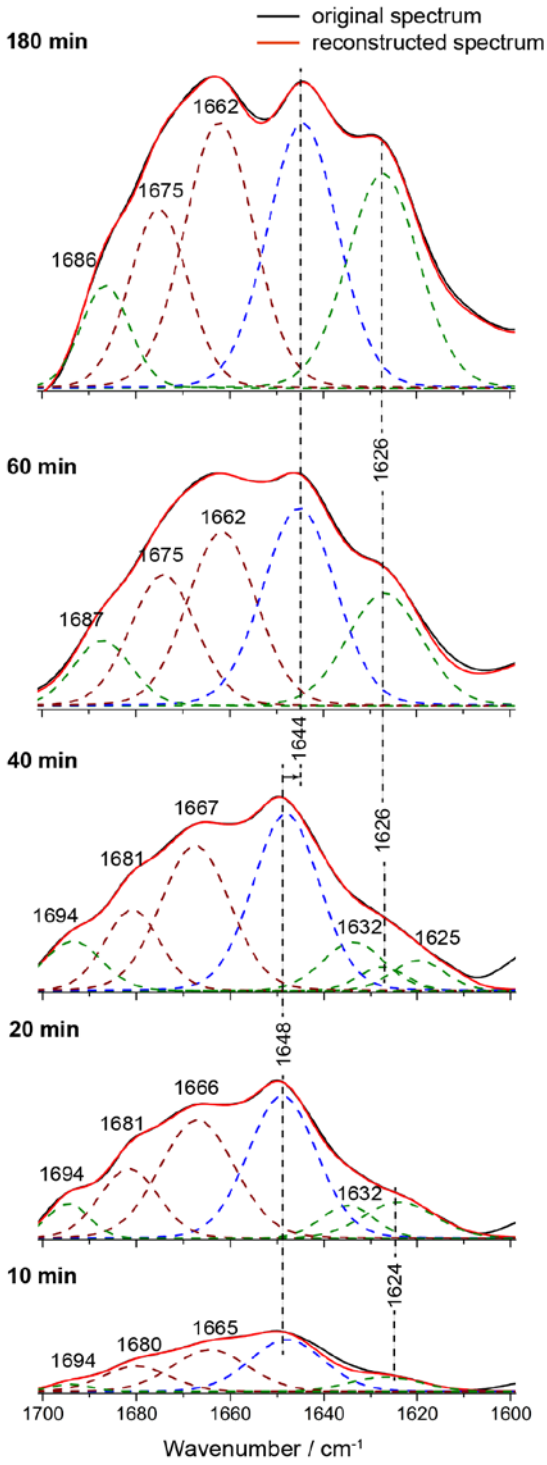

Figure S5. Curve-fitting and amide I components of N17-Q38-Flag in dependence of time (10 min, 20 min, 40 min, 60 min and 180 min after enzymatic cleavage with Ulp1). The spectra show structural transitions of the N17-Q38-Flag fragments. The early spectra (10 and 20 min) reveal that intermolecular β-sheets (1624 cm^{-1}) but also intramolecular β-sheets (1632 cm^{-1}) are formed with a sequence length of 38 glutamines. The band component at 1632 cm^{-1} can clearly be identified in the second-derivative spectrum (Fig. 6, main text) and is not present for N17-Q11-Flag. After 40 min, one band at 1626 cm^{-1} develops showing that rearrangements take place, tentatively assigned to the growth of an extended β-structured fibril with antiparallel β-sheet organization (1694/1686 cm^{-1}). There is a significant fraction of disordered structure (1648/1644 cm^{-1}) and loops/turns (1660/1662 cm^{-1}) which contribute to the final aggregates. Small band shifts indicate slight structural rearrangements of the secondary structure elements.

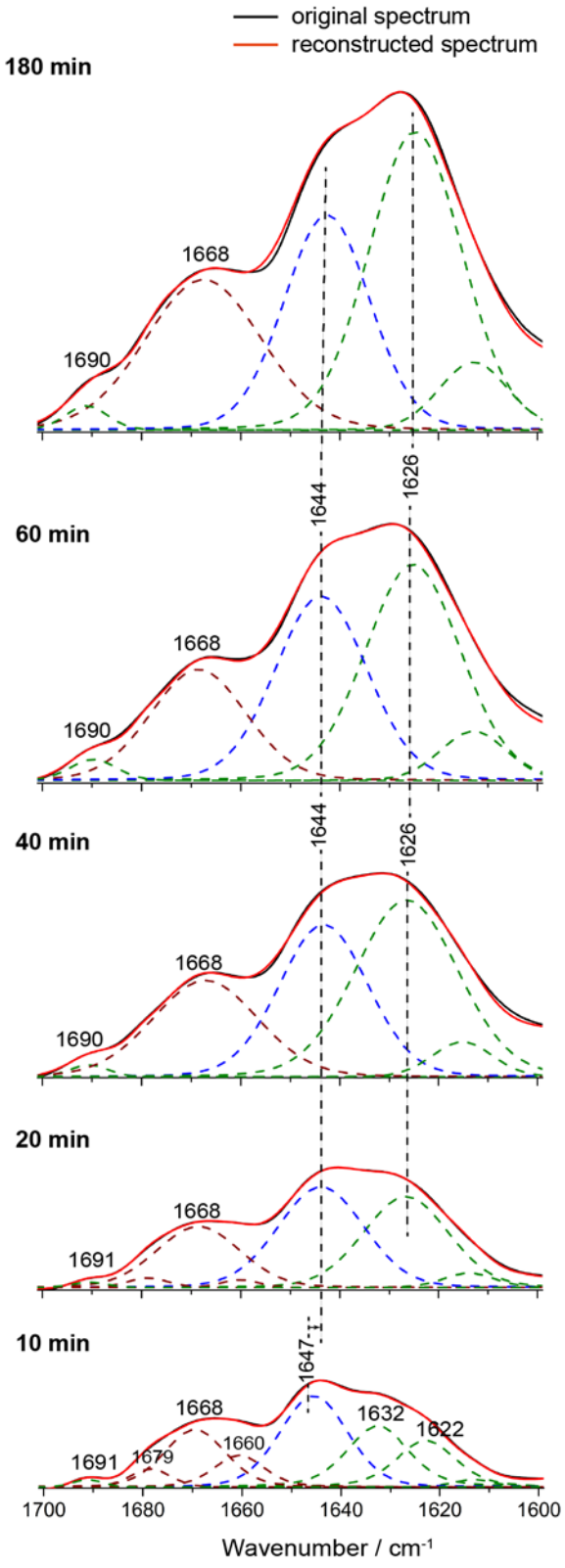

Figure S6. Curve-fitting and amide I components of N17-Q56-Flag in dependence of time (10 min, 20 min, 40 min, 60 min and 180 min after enzymatic cleavage with Ulp1). The spectra show the structural transitions of the N17-Q56-Flag fragments. Intermolecular (1622 cm^{-1}) and intramolecular (1632 cm^{-1}) β-sheet organizations are already present after 10 min. After 40 min, one band at 1626 cm^{-1} develops showing that rearrangements take place, tentatively assigned to the growth of an extended β-structured fibril. The bands at 1691/1690 cm^{-1} confirm the antiparallel orientation. Disordered structure (1647/1644 cm^{-1}) as well as loops/turns (1679-1660 cm^{-1}) contribute to the aggregates, however the relative intensities indicate that the β-structure dominates in the final aggregates in contrast to N17-Q38-Flag.

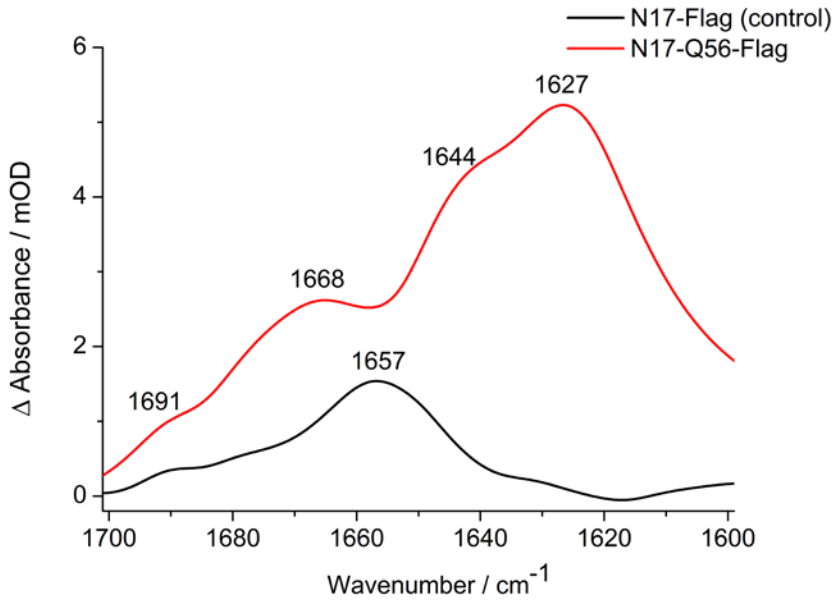

Figure S7. Amide I spectrum of N17-Flag (black) released upon Ulp1 cleavage from the control construct (no glutamine sequence) in comparison to polyQ56 (red). Both spectra were recorded after 300 min of Ulp1 incubation. It becomes obvious that no bands were observed for the control N17-Flag which would refer to any β-structured aggregate as discussed in the main text. The weak band at 1657 cm^{-1} was assigned to the α-helical structure of N17 which undergoes marginal conformational changes (when N17-Flag is released into the solution) as compared to the conformational changes of the glutamine sequence. Thus this band does not contribute to the curve-fitting and amide I components of the N17-Q_n-Flag spectra (Fig. S4, S5, S6).

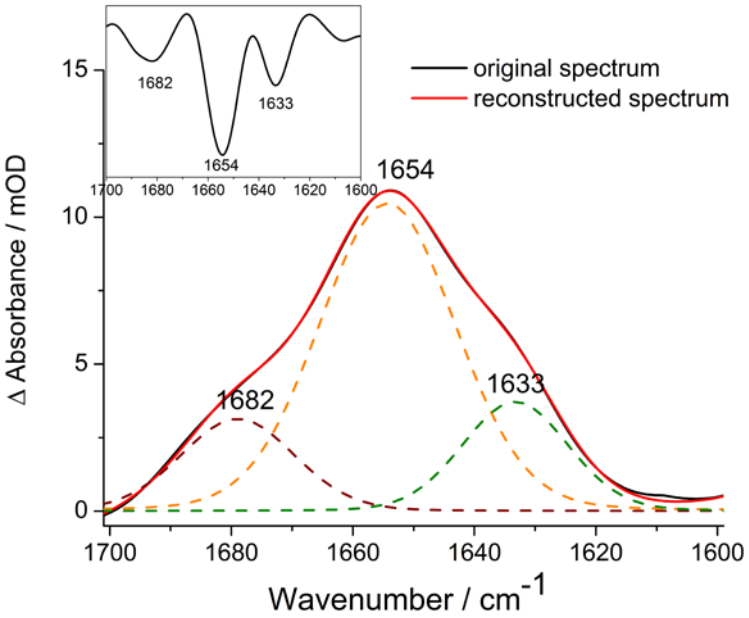

Figure S8. Curve-fitting and amide I components of the Ulp1 protease. Ulp1 was immobilized to the LB via its His-tag. The spectrum of the LB with the H_2O/buffer was taken as background. The second- derivative spectrum (inset) reveals the peak positions of the amide I components used in the curve-fitting procedure. The protease has a high amount of α-helical structure (1654 cm^{-1}) and a small contribution of intramolecular antiparallel β-sheet structure (1633/1682 cm^{-1}). The IR secondary structure analysis agrees reasonably well with the high-resolution structure determined by X-ray crystallography (3).

Supporting References

1. Rigler, P., W.-P. Ulrich, P. Hoffmann, M. Mayer, and H. Vogel. 2003. Reversible immobilization of peptides: Surface modification and in situ detection by attenuated total reflection FTIR spectroscopy. ChemPhysChem 4:268-275.
2. Ding, H., Y. Xu, Q. Chen, H. Dai, Y. Tang, J. Wu, and Y. Shi. 2005. Solution structure of human SUMO-3 C47S and its binding surface for Ubc9. Biochemistry 44:2790-2799.
3. Mossessova, E., and C. D. Lima. 2000. Ulp1-SUMO crystal structure and genetic analysis reveal conserved interactions and a regulatory element essential for cell growth in yeast. Mol Cell Vol. 5:865–876.